

Anisotropic Hydrodynamic Parameters of Regenerator Materials Suitable for Miniature Cryocoolers

T.J. Conrad¹, E.C. Landrum¹, S.M. Ghiaasiaan¹, C.S. Kirkconnell²,
T. Crittenden³, and S. Yorish³

¹Georgia Institute of Technology, Atlanta, GA 30332

²Raytheon SAS, El Segundo, CA 90245

³Virtual AeroSurface Technologies, Atlanta, GA 30318

ABSTRACT

Recent successful CFD models of cryocooler systems have shown that such models can provide very useful performance predictions for cryocoolers. For miniature cryocoolers, CFD modeling is likely the best technique available as models developed for larger systems may not accurately represent phenomena which become important as the device scale is reduced. Accurate CFD modeling of Stirling and pulse tube refrigerators requires realistic closure relations, particularly with respect to the hydrodynamic and thermal transport processes for the porous media which make up their heat exchangers and regenerators. Generally, these porous media are morphologically anisotropic, and thus the parameters which characterize them are anisotropic as well. Measurement of the hydrodynamic parameters in at least two dimensions is therefore preferred.

Miniature regenerative cryocoolers will require porous regenerator and heat exchanger fillers with considerably smaller characteristic pore sizes than those commonly used in larger scale devices. This paper describes measurements of the hydrodynamic parameters of stacked discs of 635 mesh stainless steel and 325 mesh phosphor bronze using a CFD-assisted methodology. These materials are among the finest commercially available structures and can be suitable for use as miniature regenerator and heat exchanger fillers. Measurements were made in the axial and radial directions for both steady and oscillatory flow. Higher frequency operation is preferred for miniature cryocoolers; therefore a frequency range between 50 and 200 Hz was investigated for the oscillatory flow cases. The test setups for steady flow incorporated static pressure transducers and a mass flow rate meter; for oscillatory flow, the apparatus included dynamic pressure transducers and hot wire probes for CFD model verification. These test setups were each modeled using the Fluent CFD code. The directional Darcy permeability and Forchheimer's inertial coefficients were obtained based on iterative comparisons between experimental measurements and CFD simulation results.

INTRODUCTION

Computational fluid dynamics (CFD) modeling of pulse tube refrigerators requires realistic closure relations, particularly with respect to the hydrodynamic and thermal transport processes for

the porous media which constitute a cryocooler's regenerator and heat exchangers. Useful experimental data and correlations have been published recently for some widely used regenerator fillers.¹⁻⁴ These fillers, however, may not be appropriate for miniature cryocoolers due to their relatively coarse structure. Therefore, experimental measurements were performed to determine the hydrodynamic parameters of stacked screens of stainless steel 635 mesh and phosphor bronze 325 mesh, some of the finest commercially available materials suitable for use in miniature cryocoolers.

It should be emphasized that without direct pore-level simulation, the macroscopic conservation equations which govern fluid flow through the porous media require empirical momentum closure parameters, and experimental data is needed for the development of these empirical correlations.¹⁻³ These empirical correlations include the Darcy permeability and Forchheimer's inertial coefficient which are needed for the closure of macroscopic momentum conservation equations. Generally, the porous media that are encountered in cryocoolers are morphologically anisotropic, and thus the parameters which characterize them are anisotropic as well. Measurement of the hydrodynamic parameters in at least two dimensions is therefore preferred. Hydrodynamic parameters may also vary when these fillers are subjected to steady or periodic flows. Therefore resistance parameters were found for steady as well as steady-periodic or oscillatory flow conditions. The directional hydrodynamic flow resistance parameters are determined here using experimental measurements of the fluid mass flow rate and the pressure drop across the porous media. By simulating the experimental test sections using a CFD tool we could iteratively adjust the viscous and inertial flow resistances until agreement is reached between simulated and experimental results.

The hydrodynamic parameters of stacked discs of 635 mesh stainless steel wire cloth and 325 mesh phosphor bronze wire cloth were thus determined using experimental data and a CFD assisted method. Wire cloth material was supplied from TWP Inc., and test samples were machined by Virtual AeroSurface Technologies using a punching operation. Measurements were made in the axial and radial directions for both steady state and oscillatory flow conditions. Higher frequency operation is preferred for miniature cryocoolers; therefore a frequency range between 50 and 200 Hz was investigated for the oscillatory flow cases. Research grade helium at room temperature (24°C) with a nominal purity of 99.9999% was used in all the tests as the working fluid. This system of formulating hydrodynamic characteristics is comparable to that used by Cha¹ and Clearman.²

PARAMETER DETERMINATION

Steady Flow Experiments

Diagrams of the steady flow axial and radial test setups are shown in Figures 1 and 2, respectively. The experimental and computational procedures for determining the hydrodynamic steady, axial and radial flow resistances were very similar. Equipment utilized in both cases is identical, with the exception of the porous test section, sample housing and its associated fittings and sensor mounts.

The steady flow experimental apparatus consisted of a helium supply tank and pressure regulator, two Paine Electronics Series 210-10 static pressure transducers, a Sierra Instruments 820 Series

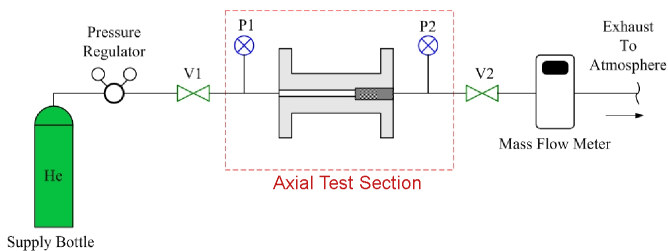


Figure 1. Steady axial flow experimental setup.

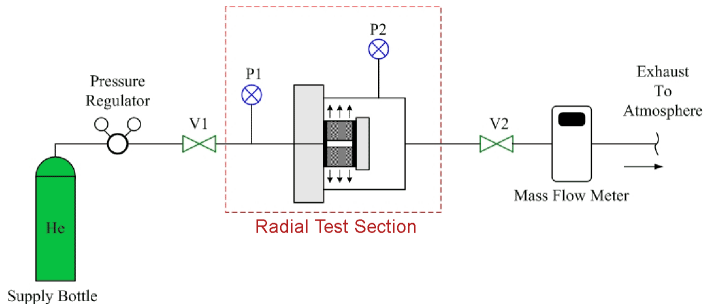


Figure 2. Steady radial flow experimental setup.

Top-Trak mass flow meter, a specially designed test section containing the porous sample and the associated piping and Swagelok fittings and valves. Pressure signals were amplified and calibrated through an Omega DMD-465WB signal conditioner. The static pressure transducers and mass flow meter each have an accuracy of $\pm 0.25\%$ and $\pm 1.5\%$ of full scale, respectively. Pressure and mass flow rate measurements were read as analogue voltage signals via handheld digital multimeters.

The axial flow test section which houses the porous media is a hollow aluminum cylinder with an inner diameter of 0.158 in (4.013 mm). End pieces bolted onto flanges located on either side of the test section constrain the porous samples and provide a mount for one of the static pressure transducers. The test sample and housing were specifically designed with a large aspect ratio of 3.175 to ensure that the flow had a predominant axial velocity component; so that the flow in the radial direction can be considered small. Each porous sample was fabricated with a strict tolerance to ensure negligible clearance between its circumference and the inside of the test section.

The radial test section contains an annular ring of the porous media of interest mounted onto an aluminum slab constrained by a cap, nuts and three threaded rods. Radial test samples were specifically designed to produce a predominately radial flow regime within the porous media. Rubber gaskets on either side of the porous material ensure that all the mass flux passes in the radial direction through the inner diameter and exits through the outer diameter. The length of the annular porous sample is adjusted by tightening the nuts on the threaded rods to closely match the porosity of its axial counterpart.

Important details including wire diameter, pore size and sample porosity of axial and radial test pieces utilized in both the steady and oscillatory flow cases are summarized in Table 1.

In axial and radial steady flow setups valves, V1 and V2, and the static pressure transducers, P1 and P2, are respectively located upstream and downstream of the test section. During each steady flow test, helium flows from the charged bottle through the pressure regulator, past the valve V1 and into the test section. The fluid then leaves the test section through valve V2 and is straightened before it passes through the mass flow meter before it is exhausted to the atmosphere. Each test run was performed only after strict assurance of a hermetically sealed setup. With valve V2 closed and valve V1 open, the system was charged to a supply pressure of 400 psig (2.86 MPa). Valve V2 was then modulated to offer a suitable range of mass flow rates. Static pressures P1 and P2 were recorded for each distinct flow rate. In order to prevent a large fluctuation in mean pressure through-

Table 1. Steady and oscillatory test sample details.

Porous Media	Sample Geometry			Mesh Geometry		Measured Porosity ---
	I.D. mm	O.D. mm	Length mm	Wire Dia micron	Pore Size micron	
Axial Samples						
325 Phosphor Bronze	-	4.0	12.7	35.6	43	0.674
635 Stainless Steel	-	4.0	12.7	20.3	20	0.631
Radial Samples						
325 Phosphor Bronze	4.0	20.0	3.4	35.6	43	0.670
635 Stainless Steel	4.0	20.0	6.1	20.3	20	0.630

out each sample run, a maximum allowable change in pressure across the test section was limited to 100 psi (0.69 MPa). For each test run, pressure drops between static pressures P1 and P2 were then plotted against mass flow rate. In order to simplify the data analysis, axial – flow experimental data for each filler material was curved fitted to a 5th order polynomial while radial test points were fitted to a 2nd order polynomial. Each curve fit was constrained with a zero intercept and would act as a guide for defining the boundary conditions to be used for CFD simulations.

Steady Flow Simulations and Data Analysis

Based upon the aforementioned experimental curve fit polynomials, seven representative experimental data points across the full range of mass flow rates were then input to the Fluent CFD code, providing for the indirect solution of hydrodynamic viscous and inertial resistances. The simulations used a two – dimensional, axisymmetric mesh that modeled the geometry of the experimental test setup from stations P1 to P2. In all the simulations, helium was treated as an ideal gas with constant viscosity. Multiple nodal networks of varying grid sizes were developed to examine the effect of mesh size on the simulation outcomes. A mesh with the smallest number of nodes which led to reasonable mesh size independent of results was eventually specified and applied, affording efficient use of computational time.

A single Fluent case was created for each representative data point and experimentally-measured parameter values were input as boundary conditions for simulations. A mass flow rate boundary condition was used at the inlet while a pressure outlet boundary condition was implemented downstream at the P2 location. The model's viscous and inertial resistances were iteratively changed until there was agreement between the simulated area-weighted static pressure at the inlet and experimental static pressure at P1 at all chosen data points.

Although turbulent flow was not expected in the porous section, Reynolds numbers in some open sections were high enough to imply turbulent flow. As a result, the Reynolds–Averaged Navier Stokes $k-\epsilon$ turbulence model was used in the steady axial simulations. However, conditions within the radial test section permitted a laminar flow model in the steady radial flow simulations.

For both the axial and radial steady flow cases, the viscous resistance could be determined at low flow rates because inertial effects were small. A trial and error method was used until a unique viscous resistance satisfied the first several data points of the low flow regime. This term was then fixed and only the inertial resistance was adjusted in the subsequent simulations. This method of predetermining the viscous resistance was applied to both axial and radial steady flow regimes and was modified slightly for oscillatory cases. The iterative process was continued until good agreement was achieved between simulated and experimental pressure drops across the entire range of mass flow rates.

Oscillatory Flow Experiments

Diagrams of the oscillatory – flow axial and radial tests setups are shown in Figures 3 and 4, respectively. The experimental and computational procedures for determining the hydrodynamic axial and radial flow resistances for oscillatory flow were very similar. The equipment utilized in both cases is identical, with the exception of the porous test section, the sample housing and its associated fittings and sensor mounts.

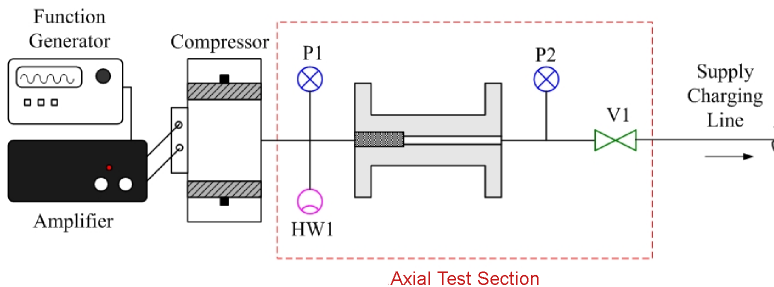


Figure 3. Oscillatory axial flow experimental setup.

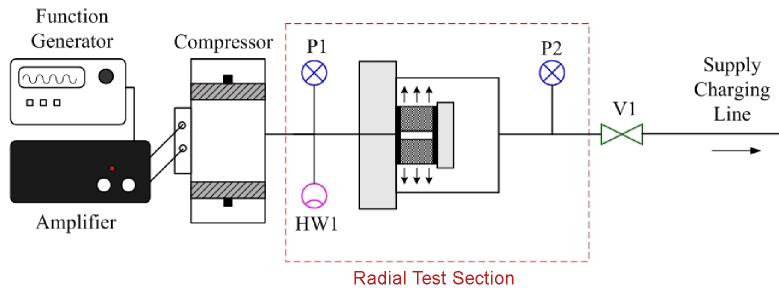


Figure 4. Oscillatory radial flow experimental setup.

The oscillatory flow experimental setups consisted of a Hughes Aircraft Tactical Condor compressor, HP-Agilent 33120A function waveform generator and HP-Agilent 3852A data acquisition control unit, Crown DC-300A Series II amplifier, a constant-temperature hot wire anemometer (HWA) with a TSI Flowpoint 1500 Series signal conditioner, two high frequency PCB Piezotronics 101A05 dynamic pressure transducers, a specially designed test section containing porous media and the associated piping, fittings and a helium charge tank. The dynamic pressure transducers have a resolution of 2 mpsi (0.014 kPa). Hot wire calibration curves were obtained at 2.86 MPa (400 psig) and 500 psig (3.45 MPa) under steady flow conditions in an inline fitting using a mass flow meter. An HP VEE virtual console was operated to integrate all sensor measurements and store their output data. An iron core transformer was also utilized to offer better power transmission from the amplifier to the compressor.

The experimental setup for periodic flow is a closed system bounded by the compressor and the valve, V1. Both the axial and radial oscillatory flow test sections consist of the same sample pieces and housing utilized in their steady flow counterparts. Dynamic pressure transducer P1 and hot wire probe HW1 are located on the compressor side of the test section while dynamic pressure transducer P2 is positioned on the opposite side of the test section.

For the axial case, pressure sensors and HWA are mounted onto end pieces adjoining the sample housing while in the radial test setup the transducers are installed via inline fittings. Axial sensor mounts on either side of the cylindrical housing are also internally fitted with an 8.0° sloped transition cone located between the porous media and sensor tap locations. This transition is meant to avoid a large step change in pipe diameter and acts to reduce flow disturbance, resulting in an unwavering hot wire signal.

A sinusoidal signal sent to the compressor is amplified to provide the largest stable pressure oscillation at each discrete frequency. Waveforms from the hotwires are directly recorded to compare with the Fluent model results, while the periodic pressures are represented by their first three harmonics, calculated using a fast Fourier transform (FFT) following the method described by Cha.^{1,3} Data was taken at seven distinct frequencies in the 50 to 200 Hz range, in intervals of 25 Hz, at operating pressures of approximately 2.86 MPa and 3.55 MPa (400 and 500 psig). High charge pressures and high operating frequencies were selected because they are expected to apply to miniature cryocoolers.

Oscillatory Flow Simulations and Data Analysis

The experimental test section geometry between pressure transducer P1 and valve V1 is modeled by a two-dimensional axisymmetric mesh, and is simulated using the Fluent CFD code assuming laminar flow regime. A user defined oscillatory pressure inlet boundary condition is applied at P1 based upon the aforementioned Fourier series representation of the experimental measurements. Like its steady state counterpart, the viscous resistance was initially determined at 50 Hz low flow conditions, where inertial effects were considered small. Once a range of prescribed viscous resistances were established, inertial resistances were added.

The iterative determination of the viscous and inertial resistances was similar to the aforementioned steady flow tests. Accordingly, the viscous resistance term was first quantified using experi-

mental data with low flow conditions. Subsequently, the viscous resistance coefficient was kept constant while the inertial resistance term was iteratively adjusted until agreement was achieved between the simulated area-weighted static pressure at P2 and experimentally measured static pressure at that location. The periodic flow axial hydrodynamic parameters were further validated by comparing experimental velocity data from HW1 to simulated centerline velocity magnitudes at the same location. This data, however, is not presented in this paper.

RESULTS

The volume-averaged momentum conservation equation for flow through a porous medium can be written⁵ as:

$$\frac{\partial}{\partial t}(\epsilon \rho \bar{u}) + \nabla \cdot (\epsilon \rho \bar{u} \bar{u}) + \epsilon \nabla P + \nabla \cdot (\epsilon \bar{\tau}) - \epsilon \bar{F}_{bf} + \mu \bar{D} \cdot \bar{u} + \frac{C \rho}{2} |\bar{u}| \bar{u} = 0 \tag{1}$$

This equation, along with mass and energy conservation equations are numerically solved by the CFD code. The sample porosity is represented by ϵ while the viscous and inertial resistance coefficient tensors are \bar{D} and \bar{C} with units of 1/m² and 1/m, respectfully. Fluid density and viscosity are displayed as ρ and μ , and $\bar{\tau}$ represents the stress tensor. Thermodynamic pressure is shown with P and \bar{F}_{bf} represents the body force vectors (our particular simulations do not include any body forces or gravity). The vector \bar{u} represents the physical velocity within the porous structure. Assuming isotropic flow resistances, the viscous and inertial resistance coefficients will be scalar quantities. The last two terms in the above equation, which together represent the total resistance force, can then be used for the definition of the Darcy permeability and Forchheimer’s inertial coefficient according to:

$$\mu D \bar{u} + \frac{C \rho}{2} |\bar{u}| \bar{u} = \frac{\epsilon^2 \mu}{K} \bar{u} + \frac{c_f \epsilon^3 \rho}{\sqrt{K}} |\bar{u}| \bar{u} \tag{2}$$

$$K = \epsilon^2 / D \tag{3}$$

$$c_f = \frac{C \sqrt{K}}{2 \epsilon^3} \tag{4}$$

For steady and oscillatory flow hydrodynamic parameter determination, isotropic viscous and inertial resistances were assumed in Fluent simulations. This simplifying assumption was justified because the flow within the porous structure of each test apparatus was predominantly one-dimensional.

Steady Flow Parameters

Fluent simulations⁶ were performed for both porous structures at a supply pressure of 2.86 MPa (400 psig). Figures 5 and 6 display pressure drop as a function of mass flow rate for the two axial

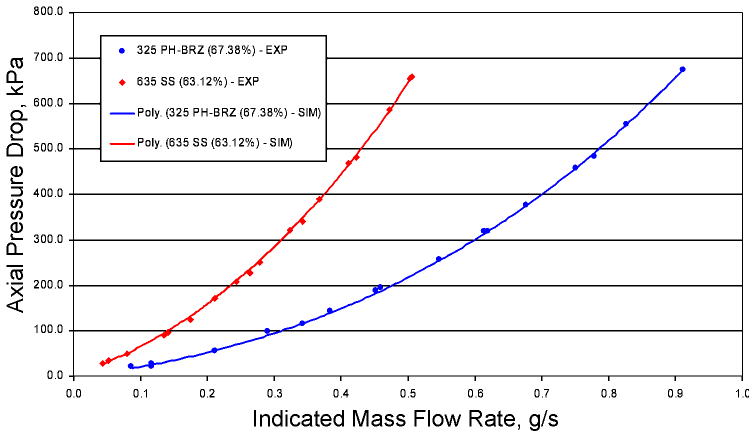


Figure 5. Steady axial flow pressure plot.

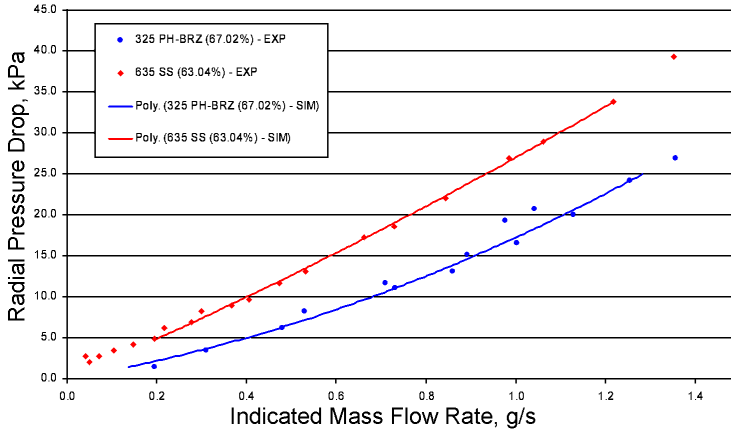


Figure 6. Steady radial flow pressure plot.

and radial flow test sections, respectively. Curves representing the simulation results are also shown along with the discrete experimental data points for comparison.

Multiple test runs were performed for each mesh filler producing mass flow rates ranging from 0.042 g/s to 1.36 g/s. The pressure drop was limited to 6.9 bar (100 psi) in each test, however. The axial steady – flow measurements were found to be well repeatable. Due to the small cross sectional area of the axial test sample and housing, large pressure drops of up to 674 kPa were recorded in those tests. As noted in Figure 5, good agreement is displayed between steady axial experimental and simulated data over the entire range of flow rates.

The approximately linear profile of the radial pressure drop plots (Fig. 6) would suggest a predominately Darcy or viscous flow pattern in these experiments, with little inertial effects.⁷ The radial flow test runs in fact produced relatively minor pressure drops, up to 40 kPa, for mass flow rates up to 1.36 g/s. As a result, some data scatter can be observed in Fig. 6.

A summary of steady flow results, including the hydrodynamic resistances, Darcy permeabilities and Forchheimer’s coefficients are provided in Table 2.

As mentioned earlier, the design of each test apparatus was expected to render the flow in the porous test section primarily one-dimensional. The CFD simulations have shown that this was indeed the case. The velocity vectors of a typical steady flow radial test run are displayed in Fig. 7. The figure shows the velocity vectors in the porous test section for the stainless steel 635 mesh filler type at a mass flow rate of 1.218 g/s. The flow is evidently predominately radial, except for the immediate vicinity of the flow area inside the annular test sample.

Oscillatory Flow Parameter

All periodic measurements were done at the largest stable input pressure amplitude based upon the compressor response. Oscillatory flows in the axial and radial directions were implemented over the frequency range of 50 to 200 Hz, at charge pressures of 2.86 and 3.55 MPa. As mentioned

Table 2. Steady flow sample hydrodynamic parameters.

Porous Media	Viscous Resistance 1/m ²	Inertial Resistance 1/m	Darcy Permeability m ²	Forchheimer's Coefficient ---
Axial Samples				
325 Phosphor Bronze	2.85E+10	28000	1.593E-11	0.183
635 Stainless Steel	9.95E+10	65000	4.004E-12	0.259
Radial Samples				
325 Phosphor Bronze	2.85E+10	58000	1.576E-11	0.382
635 Stainless Steel	1.24E+10	59000	3.205E-11	0.667

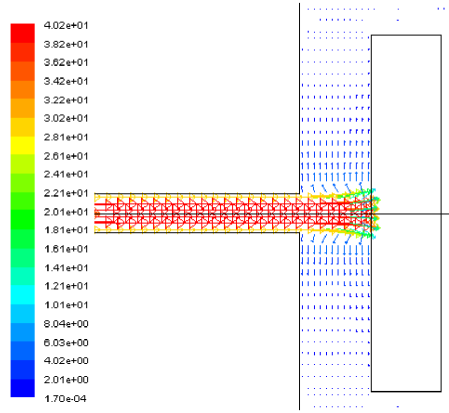


Figure 7. Velocity vectors colored by magnitude (m/s) in the radial porous section at 1.218 g/s, for the stainless steel 635 mesh filler at 63% porosity.

earlier, the viscous and inertial resistance parameters were iteratively adjusted until agreement was achieved between experimental and simulation pressure profiles at location P2. The procedure is detailed by Cha¹, and will not be repeated here. Two examples can be seen in Fig. 8, where the pressure waves of the 635 mesh stainless steel filler, at 100 Hz and 150 Hz frequencies, are displayed. The oscillatory flow hydrodynamic resistances, Darcy permeabilities and Forchheimer's coefficients are summarized in Table 3.

The results in Tables 2 and 3 confirm that the hydrodynamic resistance parameters for the tested porous structures depend on flow direction. With the exception of radial flow in 635 mesh stainless steel, the hydrodynamic resistance parameters also suggest independence of pressure. A slight dependence of these parameters on pressure can be observed for radial flow in the latter filler. In a separate investigation⁸, the present authors observed that axial steady flow hydrodynamic resistance parameters of several regenerator fillers are insensitive to average fluid pressure. The results of this investigation, although based on few experimental data, extend this observation to oscillatory flow cases with a slight exception for the unsteady radial flow in stainless steel 635 mesh filler. They also indicate that a single unique set of resistance coefficients satisfied the explored range of frequencies with only minor deviations. It should be mentioned that the hydrodynamic parameters presented in this investigation were obtained using simple graphical curve-fitting. More precise calculation of these parameters is under way by implementing a user defined function into the Fluent code that seeks porous resistances based upon optimized output variables. These calculations as well as other forms of model validation will be published in the near future. Further

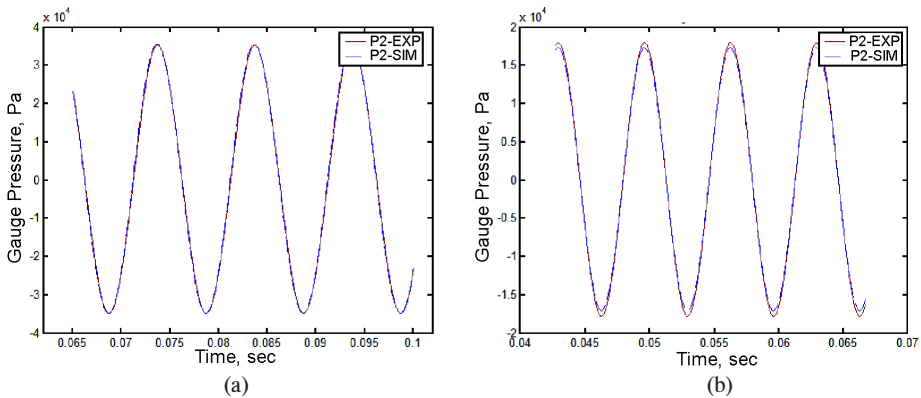


Figure 8. 635 mesh stainless steel experimental and simulated periodic axial flow pressure plots: (a) at 100 Hz and 2.86 MPa charge pressure; (b) at 150 Hz and 3.55 MPa charge pressure.

Table 3. Oscillatory flow sample hydrodynamic parameters.

Porous Media	Charge Pressure MPa	Viscous Resistance 1/m ²	Inertial Resistance 1/m	Darcy Permeability m ²	Forchheimer's Coefficient ---
Axial Samples					
325 Phosphor Bronze	2.86	1.70E+10	50000	2.672E-11	0.422
325 Phosphor Bronze	3.55	1.70E+10	50000	2.672E-11	0.422
635 Stainless Steel	2.86	9.50E+10	40000	4.194E-12	0.163
635 Stainless Steel	3.55	9.50E+10	40000	4.194E-12	0.163
Radial Samples					
325 Phosphor Bronze	2.86	2.90E+10	50000	1.549E-11	0.327
325 Phosphor Bronze	3.55	2.90E+10	50000	1.549E-11	0.327
635 Stainless Steel	2.86	1.05E+11	120000	3.785E-12	0.466
635 Stainless Steel	3.55	1.11E+11	120000	3.596E-12	0.454

experiments over a wider range of pressures and frequencies, and more porous filler types, would be required before a definitive conclusion can be made. We also recognize that the applicability of these parameters to cryogenic conditions needs experimental confirmation.

CONCLUSIONS

Hydrodynamic parameters of stacked discs of 635 mesh stainless steel and 325 mesh phosphor bronze were determined using a CFD – assisted methodology, whereby the hydrodynamic resistance parameters for these fillers are specified when they are modeled as anisotropic porous media. Measurements were made in the axial and radial directions for both steady and periodic flow conditions, for charge pressures of 2.86 and 3.55 MPa. Higher frequency operation is preferred for miniature cryocoolers, therefore periodic flow cases were performed over a frequency range between 50 and 200 Hz. Experimental test setups for steady flow included static pressure transducers and a mass flow meter; for oscillatory flow, the apparatus included dynamic pressure transducers and a hot wire probe for CFD verification. The results indicated that the Darcy and Forchheimer coefficients were generally insensitive to pressure and frequency.

REFERENCES

1. Cha, J.S., "Hydrodynamic Parameters of Micro Porous Media for Steady and Oscillatory Flow: Application to Cryocooler Regenerators," Doctoral Thesis, Georgia Institute of Technology, Atlanta, GA (2007).
2. Clearman, W.M., "Measurement and Correlation of Directional Permeability and Forchheimer's Coefficient of Micro Porous Structures Used in Pulse-Tube Cryocoolers," Masters Thesis, Georgia Institute of Technology, Atlanta, GA (2007).
3. Clearman, W.M., Cha, J.S., Ghiaasiaan, S.M., Kirkconnell, C.S., "Anisotropic Hydrodynamic Parameters of Microporous Media Applied in Pulse Tube and Stirling Cryocooler Regenerators", *Cryogenics*, Vol. 48 (2008), pp. 112-121.
4. Cha, J.S., Ghiaasiaan, S.M., Kirkconnell, C.S., "Oscillatory Flow Anisotropic Hydrodynamic Parameters of Microporous Media Applied in Pulse Tube and Stirling Cryocooler Regenerators", *Exp. Thermal Fluid Science*, Vol. 32 (2008), pp. 1264-1278.
5. Hsu, C., *Handbook of Porous Media* (2nd Ed.), Taylor and Francis Group, (2005), pp. 40-62.
6. FLUENT 6 Users Manual, Fluent Inc., 2003.
7. Wilson, L., Narasimhan, A., Venkateshan, S.P., "Permeability and Form Coefficient Measurement of Porous Inserts With Non-Darcy Model Using Non-Plug Flow Experiments," *Journal of Fluids Engineering*, Vol. 128 (May 2006), pp. 638-642.
8. Landrum, E.C., Conrad, T.J., Ghiaasiaan, S.M., Kirkconnell, C.S., "Effect of Pressure on Hydrodynamic Parameters of Several PTR Regenerator Fillers In Axial Steady Flow", *Cryocoolers 15*, ICC Press, Boulder, CO (2009), (this proceedings).